Eidgenössische Technische Hochschule Zürich
Swiss Federal Institute of Technology Zurich

Characterization of a phaseplate for the creation of a tophat potential

Semester Project

Nicolò Montalti
nmontalti@student.ethz.ch

Quantum Optics Group
Departement of Physics, D-PHYS
ETH Zürich

Supervisor:
Prof. Tilman Esslinger

Advisors:
Dr. Meng-Zi Huang
Mohsen Talebi

June 13, 2023

Abstract

Contents

Chapter 1

Introduction

Predicting the behaviour of complex systems has always been an important goal of scientific research. From predicting the motion of stars and planets in our solar system, to understanding the behaviour of complex systems showing chaotic behaviours. In history, before scientists were able to find analytical solutions to many problems, they often relied on simulations. A celebrated example are the astronomical clocks that were built in Asia and Europe in the period between 1000 and 1500, such as the famous astronomical clock in Prague (1410) or the Zytglogge in Bern (1530). They were used to predict the position of the planets and the constellations, the phases of the moon and its eclipses [1].

With the advent of quantum mechanics, a new kind of problems for which no analytical solution is possible was found. Given the high dimensionality of the Hilbert space, classical computers cannot be used to find numerical solutions to quantum many body problems. For example, simulating a system of $N = 36$ qubit using two double-precision floating-point numbers to store a complex number, would require approximately $2^{N+1} \times 8$ byte $=$ 1 Terabyte of memory. For every additional qubit, this number would double.

Richard Feynman was the first to propose to use a quantum system to handle this complexity making use of the law of quantum mechanics itself. In 1982, he proposed to make use of "one controllable quantum system [to] simulate another" [2]. In this way, a system of N quantum particles could be simulated using another system of N qubits. The problem is then moved to finding a system that can be easily tuned and controlled, such that it can be used to simulate a wide range of problems.

1.1 Analog and digital quantum simulation

Two different approaches have arisen in the past years: (digital) quantum computation and (analog) quantum simulation. In the first case, the information is encoded in qubits that can be in two computational states $|0\rangle$ and $|1\rangle$. In the latter, a direct mapping between the original problem (i.e. its Hamiltonian) and the simulating system is realized. Among the most promising platforms for quantum computation, we cite the use of superconducting circuits [3], Rydberg atoms [4] and trapped ions [5]. Whereas for quantum simulation, the use of ultracold quantum gases has become increasingly popular [1].

For example, a system of electrons moving in an ionic periodic lattice potential, can be simulated using a gas of fermionic atoms trapped in an optical lattice potential. Here, the periodic potential through which the particles move is generated externally by making use of the interference pattern of overlapping laser beams [6]. It is performing an experiment of this kind that Bloch oscillations, predicted in 1929 by Felix Bloch [7], were directly observed in 1996 in a cloud of ultracold Caesium atoms [8], after being observed in 1992 through the emission of THz radiation by the electrons in a semiconductor super lattice [9].

In the following years, new interesting experiments were proposed to simulate the behaviour of different quantum systems. Among them, we cite the use of optical lattices to investigate insulating and superfluid quantum phases [10], the use of cavities to mediate long range interactions [11] and the observation of quantized conductance in neutral matter [12]. We will focus on this last experiment, since my project was related to it.

1.2 Transport experiments

Transport experiments study the transport properties of particles moving from one reservoir to another. Krinner *et al.* reported the observation of quantized conductance in the transport of neutral atoms driven by a chemical potential bias [12]. Their experiment let them investigate quantum conductors with wide control not only over the channel geometry, but also over the reservoir properties, such as interaction strength, size and thermalization rate.

The basic setup of the experiment is shown in Fig. 1.1. A cloud of atoms is radially trapped with a dipole trap realized with a red-detuned laser. Along the y axis the confinement is produced by the magnetic field curvature of the Feshbach coils. This defines a cigar-shaped cloud elongated in the y direction. The cloud is then split in two reservoir connected by a quasi-2D channel sending a blue-detuned TEM_{01} laser mode in the x direction. The blue-detuned laser creates a repulsive potential that confines the atoms in a quasi-2D region. The experiment is then carried on creating a chemical potential imbalance between the two reservoir and studying the conduction of atoms between them. Different experiments can be realized creating a temperature imbalance or a spin imbalance between the reservoirs.

The focus of this thesis is on the blue-detuned laser generating the 2D channel. In the current experiment, the laser is in a TEM_{01} mode. The beam is shaped through a series of optical components shown in Fig. 1.2. It is clear that the potential inside the channel region is not uniform along the y direction. The conductance is influenced by this varying potential and it would be desirable to have a uniform region connecting the two reservoir.

The opportunity to create such a uniform 2D channel was previously investigated by

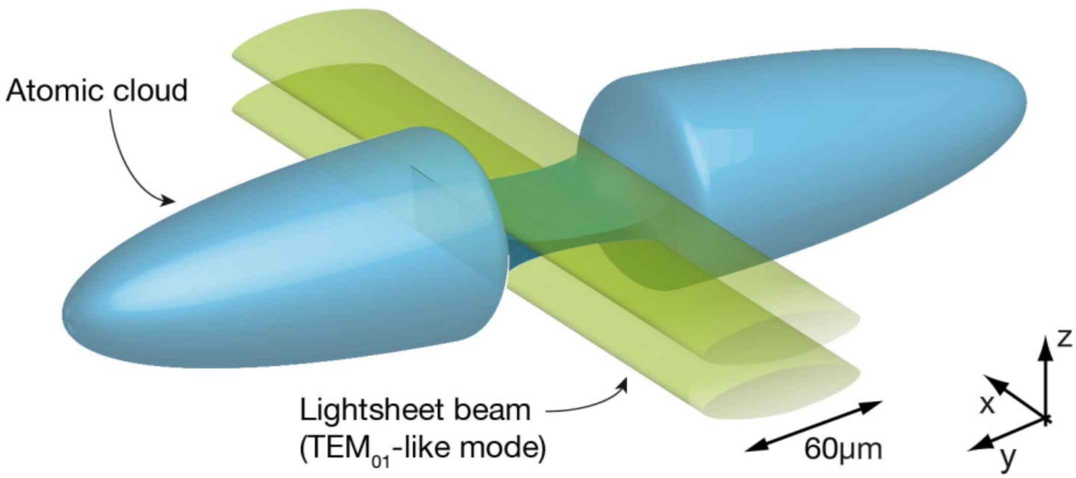

Figure 1.1: *Experimental setup. A cloud of atoms is trapped in a cigar-shaped potential. A blue-detuned TEM_{01} laser mode propagating in the x direction defined a quasi-2D channel connecting two smoothly connected reservoirs. Figure from Krinner [12].*

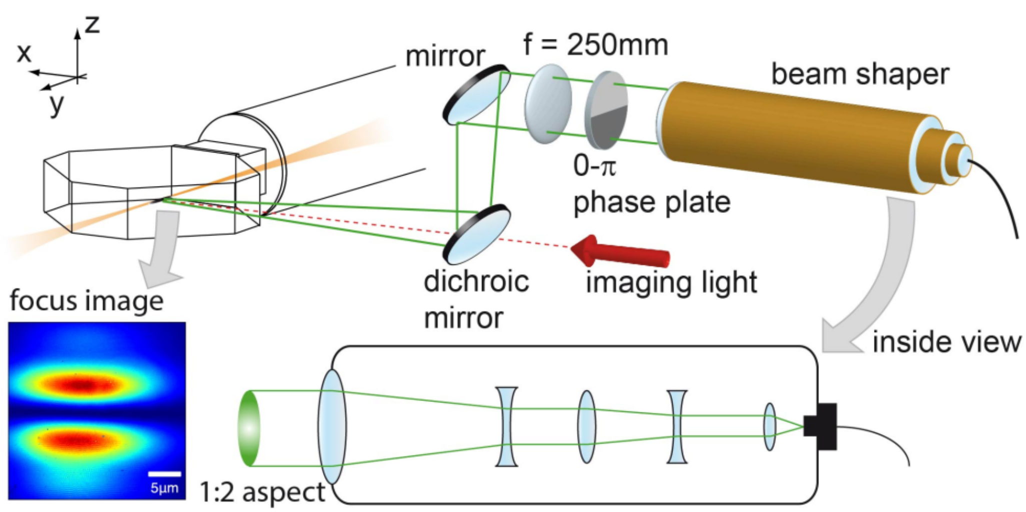

Figure 1.2: *Generation of the TEM_{01} mode for the creation of 2D channel. A set of spherical and cylindrical lenses is used to expand the beam in the z direction. The beam is then sent to a $0-\pi$ phase plate and focused through a 250 mm lens on the atomic cloud. Figure from Krinner [12].*

Moritz Schmidt in his semester project [13]. Schmidt considered two options for generating a uniform light sheet: the use of liquid-crystal spatial light modulators and of custom-made glass $0-\pi$, top-hat phase-plates. It was found that this second option is more suitable to the experiment, being at the same time able to satisfy the experimental requirements and considerably cheaper.

1.3 Outline

In this report, I analyse and characterize the custom-made phase plate ordered for the creation of the uniform light sheet. I will start by reviewing the theory behind spatial light modulation, focusing on how a phase plate can be used to shape light beams. Then I will present the apparatus used to characterize the phase plate and the results.

Chapter 2

Theoretical background

In this chapter we focus on how we can generate an arbitrary potential for our cloud of ultracold atoms. To understand it, we first need to review the basics of quantum optics that explain how atoms and light interact, resulting in a dipole force that can be used to trap the atoms. We then focus on the theory of spatial light modulation. For it, we will present a discussion on Fourier optics and use it to understand how a phase plate can be used for such a purpose.

2.1 Atom-light interaction

It is well known that atoms can interact with light. At the quantum level, the interaction is usually interpreted as the absorption or emission of photons by the atoms. Despite this picture being accurate, matter can also interact with light through virtual absorption or emission processes, that result in interesting behaviours. For this to happen, the frequency of light must be far detuned from the excitation energy of the atoms. An important effect of this type of interaction is the dipole force exerted by light on atoms. To understand the origin of this force, it is sufficient to remember that photons, besides energy, also carry momentum. When a photon is scattered by an atom, its momentum is transferred, generating an effective force that acts on the latter.

2.1.1 The dipole force

To study this force in more detailed, we model the atom as a two level system, where the energy levels are separated by an energy $\hbar\omega_{eg}$. We also consider light made of a single mode of frequency $\omega/2\pi$, like the light emitted by a laser. The following discussion is adapted from Jonathan Home's lecture notes on Quantum Optics.

We start by writing the interaction Hamiltonian in the dipole approximation

$$H_{\text{int}} = \boldsymbol{d} \cdot \boldsymbol{E}(\boldsymbol{r}) \tag{2.1}$$

where $\boldsymbol{d}$ is the dipole moment operator, $\boldsymbol{E}$ the electric field and $\boldsymbol{r}$ the position of the atom. The Hamiltonian of the atom without the interaction term is

$$H_0 = \frac{\hbar\omega_{eg}}{2}\sigma_z + \frac{\boldsymbol{p}^2}{2m} \tag{2.2}$$

where σ_z is the third Pauli matrix and $\boldsymbol{p}$ is the momentum operator. Furthermore, we consider a classical electric field

$$\boldsymbol{E} = \frac{1}{2}E_0 f(\boldsymbol{r})\left(e^{i(\boldsymbol{k}\cdot\boldsymbol{r}-\omega t)} + e^{-i(\boldsymbol{k}\cdot\boldsymbol{r}-\omega t)}\right)\boldsymbol{\epsilon} \tag{2.3}$$

where E_0, ω and $\boldsymbol{\epsilon}$ are the field strength, frequency and polarization respectively. The function $f(\boldsymbol{r})$ allows the field amplitude to vary spatially. The interaction Hamiltonian can be rewritten as

$$H_{\text{int}} = (\boldsymbol{\mu}_{eg}\cdot\hat{\boldsymbol{\epsilon}}E_0)\frac{f(\boldsymbol{r})}{2}(\sigma_+ + \sigma_-)\left(e^{i(\boldsymbol{k}\cdot\boldsymbol{r}-\omega t)} + e^{-i(\boldsymbol{k}\cdot\boldsymbol{r}-\omega t)}\right) \tag{2.4}$$

where $\mu_{eg} = \langle e|\,\boldsymbol{d}\,|g\rangle$. It is useful to move to the rotating frame with respect to the laser frequency. After transforming the Hamiltonian and performing the rotating wave approximation, we are left with

$$H = -\frac{\hbar\delta}{2}\omega_z + \frac{\boldsymbol{p}^2}{2m} + \frac{\hbar\Omega(\boldsymbol{r})}{2}\left(\sigma_+ e^{i\boldsymbol{k}\cdot\boldsymbol{r}} + \sigma_- e^{-i\boldsymbol{k}\cdot\boldsymbol{r}}\right) \tag{2.5}$$

with $\Omega(\boldsymbol{r}) = \boldsymbol{\mu}_{eg}\cdot\hat{\boldsymbol{\epsilon}}E_0 f(\boldsymbol{r})/\hbar$ and $\delta = \omega - \omega_{eg}$.

We can find the resulting force applied on the atom by using Heisenberg's equation of motion

$$\begin{aligned}\boldsymbol{F} = \frac{\mathrm{d}\boldsymbol{p}}{\mathrm{d}t} &= \frac{i}{\hbar}[H,\boldsymbol{p}] \\ &= -\frac{\hbar}{2}\nabla\Omega(\boldsymbol{r})\left(\sigma_+ e^{i\boldsymbol{k}\cdot\boldsymbol{r}} + \sigma_- e^{-i\boldsymbol{k}\cdot\boldsymbol{r}}\right) - \frac{\hbar}{2}\Omega(\boldsymbol{r})i\boldsymbol{k}\left(\sigma_+ e^{i\boldsymbol{k}\cdot\boldsymbol{r}} - \sigma_- e^{-i\boldsymbol{k}\cdot\boldsymbol{r}}\right)\end{aligned} \tag{2.6}$$

We observe that we get two terms. The first, proportional to the spatial derivative of the field strength, includes a contribution in phase with the light field. It is the term that results in the dipole force exerted by the field on the atom, the one we are interested in. The second term is proportional to the field strength, and it is out of phase of a factor of π with respect to the field. It is responsible for the scattering force, essential for cooling atoms. The second term is dominated by the first for large detuning δ, and it will then be neglected in the following discussion.

We will now make use of two approximation to simplify the calculations. We first make use of a mean-value approximation for the centre-of-mass degree of freedom. This means that we evaluate the internal states operators appearing in $\mathrm{d}\boldsymbol{p}/\mathrm{d}t$ using the mean position $\boldsymbol{r} = \langle\boldsymbol{r}\rangle + \langle\boldsymbol{v}\rangle t$, where $\boldsymbol{v}$ is the velocity of the atom. Moreover, since the timescale on which the internal degrees of freedom of the atom evolve are much faster than the timescale associated to the movement of it, we only consider the steady state solution of the atomic dynamics.

Making use of the approximations explained above, in the limit $\delta \gg \Omega, \Gamma$, where Γ is the decay rate, we find

$$\boldsymbol{F}_{\mathrm{dip}} = \left\langle \frac{\mathrm{d}\boldsymbol{p}}{\mathrm{d}t} \right\rangle = -\frac{\hbar}{2}\frac{\Omega}{\delta}\nabla\Omega \tag{2.7}$$

We notice that the dipole force is proportional to the field strength and its gradient and inversely proportional to the detuning. Moreover, its sign depends on the sign of the detuning. Red-detuned light ($\delta < 0$) generates an attractive potential and can be used to create optical tweezers. This is exploited in our experiment for the creation of the cigar-shaped cloud. On the other hand, blue-detuned light ($\delta > 0$) generates a repulsive potential. This is what we need for the creation of the 2D channel. In the experiment, we use a 660 nm laser, blue-detuned with respect to the Lithium atomic transition of 671 nm.

2.2 Spatial light modulation

Now that we know how light interacts with atoms, we are interested in the techniques that can be used to arbitrary shape a light beam. At the basis of these techniques there is Forier optics, which will be explained in the next section. We will then look at the different tools that can be used to achieve this goal, focusing on the use of phaseplates.

2.2.1 Fourier optics

Fourier optics is essential to understanding how spatial light modulation works. The basic idea is that a lens returns the Fourier transform of an incident beam on its focal plane. This can be used to transform a phase modulation in an intensity modulation. We will now look at this concept in more detail, providing a short introduction to Fourier optics adapted from Saleh and Teich [14] and Schmidt's previous work [13].

Let's suppose we have a monochromatic wave of wavelength λ propagating in the z direction. In the $z = 0$ plane, we can denote its complex amplitude with a function $f(x, y)$. The function $f(x, y)$ can be Fourier transformed and decomposed in plane waves propagating in the x and y directions

$$f(x, y) = \int \mathrm{d}\nu_x \mathrm{d}\nu_y F(\nu_x, \nu_y) e^{-2\pi i(\nu_x x + \nu_y y)} \tag{2.8}$$

where $\nu_x = k_x/2\pi$, $\nu_y = k_y/2\pi$ and

$$F(\nu_x, \nu_y) = \int \mathrm{d}x \mathrm{d}y f(x, y) e^{2\pi i(\nu_x x + \nu_y y)} \tag{2.9}$$

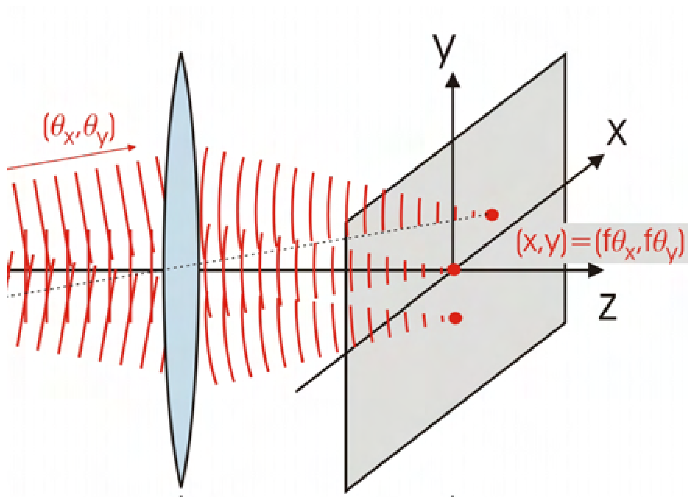

Figure 2.1: *Focusing of a plane wave into a point. A direction (θ_x, θ_y) is mapped into a point $(x, y) = (\theta_x f, \theta_y f)$. The lens in positioned at $z = 0$ and the focal plane at $z = f$. Image from Heine [15]*

.

Each plane wave travels in a direction $\theta_x = \sin^{-1}(k_x/k) = \sin^{-1}(\lambda\theta_x)$ and $\theta_y = \sin^{-1}(k_y/k) = \sin^{-1}(\lambda\theta_y)$ and has an amplitude $F(\nu_x, \nu_y)$

One way to separate the Fourier components of a wave is by using a lens. A thin spherical lens transforms a plane wave incident on it into a paraboloidal wave focused on a point on the focal plane of the lens (Saleh and Teich Sec. 2.4 [14]). As shown in Fig. 2.1, a plane wave incident at a small angle (θ_x, θ_y) if focused to the point$(x, y) = (\theta_x f, \theta_y f)$, where f is the focal length of the lens. The complex amplitude $g(x, y)$ at $z = f$ is therefore proportional to the Fourier transform of $f(x, y)$ evaluated at $\nu_x = x/\lambda f$ and $\nu_y = y/\lambda f$.

$$g(x, y) \propto F\left(\frac{x}{\lambda f}, \frac{y}{\lambda f}\right) \tag{2.10}$$

To find the proportionality factor, we trace the propagation of every plane wave in which we have decomposed the input beam through the optical system. Then we integrate over all these plane waves at the output to obtain $g(x, y)$. In the following, we will make use of the Fresnel and paraxial approximations.

A field $F(k_x, k_y)$ can be propagated from the $z = 0$ plane to $z = f$ plane by applying a phase factor $e^{-ik_z z}$

$$G(k_x, k_y) = F(k_x, k_y)e^{-ik_z z} = H(k_x, k_y, z)F(k_x, k_y) \tag{2.11}$$

with $k_z = \sqrt{k^2 - k_x^2 - k_y^2}$ and $H(k_x, k_y, z) = e^{-ik_z z}$. We can now perform the Fresnel approximation, which states that for plane waves travelling at small angles ($k_x, k_y \ll k$),

$$H(k_x, k_y, z) = e^{-ik_z z} = e^{-iz\sqrt{k^2-k_x^2-k_y^2}} \approxeq e^{-ikz} e^{i\frac{k_x^2+k_y^2}{2k}z} \tag{2.12}$$

H is defined in the Fourier space, so we can bring it back to the real space applying an inverse Fourier transform

$$h(x, y, z) = \mathcal{F}^{-1}(H(k_x, k_y, z)) = \frac{i}{\lambda z} e^{-ikz} e^{ik\frac{x^2+y^2}{2z}} \tag{2.13}$$

Now we have to take into account the effect of the lens on the beam. A parabolic lens of focal length f will apply a phasor $\phi(x, y) = \exp\left(-ik\frac{x^2+y^2}{2f}\right)$ in addition to the phase acquired by the propagation of the beam. Overall, at $z = f$

$$g(x, y) = h(h, y, f) \otimes [\phi(x, y)f(x, y)] = \frac{i}{\lambda f} e^{-ikf} F\left(\frac{x}{\lambda f}, \frac{y}{\lambda f}\right) \tag{2.14}$$

The proportionality factor is therefore found to be $1/\lambda f$ and the intensity $I(x, y)$ at the focal plane

$$I(x, y) = \frac{1}{(\lambda f)^2} \left| F\left(\frac{x}{\lambda f}, \frac{y}{\lambda f}\right) \right|^2 \tag{2.15}$$

To sum up, a lens returns a Fourier transform of the incident beam at a distance equal to the focal length. This can be used to modulate the intensity profile of the beam.

2.2.2 Spatial light modulators: the phase plate

The theory described above can be used as the working principle for numerous devices used for spatial light modulation. Among the ways light can be shaped, it is worth mentioning the use of acusto-optic modulators (AOMs), digital micromirror devices (DMDs), liquid crystals spatial light modulators (LC-SLMs) and phaseplates. All these options are good for different purposes. The first three have the advantages to be controllable, allowing the creation of arbitrary shapes simply changing the input signal.

The use of an LC-SLM for the creation of a uniform light sheet was investigated by Schmidt in his semester project [13]. However, it was found that a phase plate would offer a cheaper and more reliable alternative. These advantages come at the cost of not having the possibility to change phase profile at a later moment.

The working principle of a phase plate is very simple. A wave travelling in a transmissive medium has a lower speed than a wave travelling in air. Designing a plate with variable thickness, it is possible to imprint an arbitrary phase to a beam. The points where the plate is thicker will be delayed with respect to the points where it is thinner. Placing a lens after the plate will result in the desired intensity modulation on the focal plane.

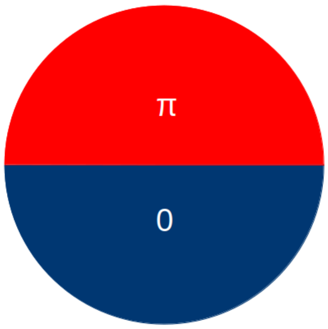

(a) $0 - \pi$ *phase plate*

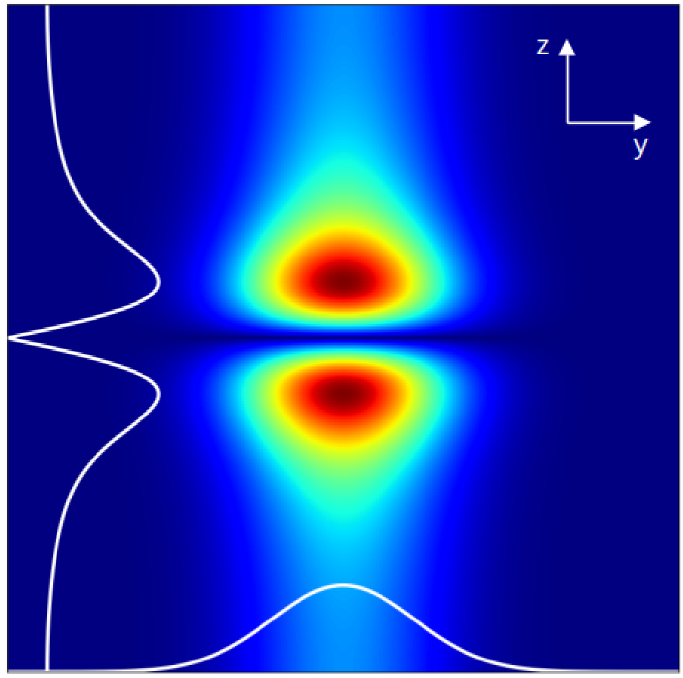

(b) *TEM*$_{10}$ *mode*

Figure 2.2: *TEM*$_{10}$ *mode generated by o* $0-\pi$ *phase plate. In the figure on the right, the intensity profile at the focal plane is shown together with the integrated intensity along the two axes.*

One of the simplest example of phase plates is the $0-\pi$ phase plate, shown in Fig. 2.2a. The plate is divided in two halves, with the upper half out of phase by a factor of π with respect to the lower half. The phase profile is then

$$\phi(x,y) = \begin{cases} 0 & y < 0 \\ \pi & y > 0 \end{cases} \tag{2.16}$$

This is the phase plate currently used in the experiment, and it generates the TEM_{10} mode shown in Fig. 2.2b.

As it is clear from Fig. 2.2b, the intensity (and therefore the potential) is not uniform along the y direction. On the contrary, it has Gaussian shape, with a peak at the centre. What we would like to achieve is a so-called top-hat potential, shown in Fig. 2.3. For it, a custom-made phase plate was ordered from Holoor. On

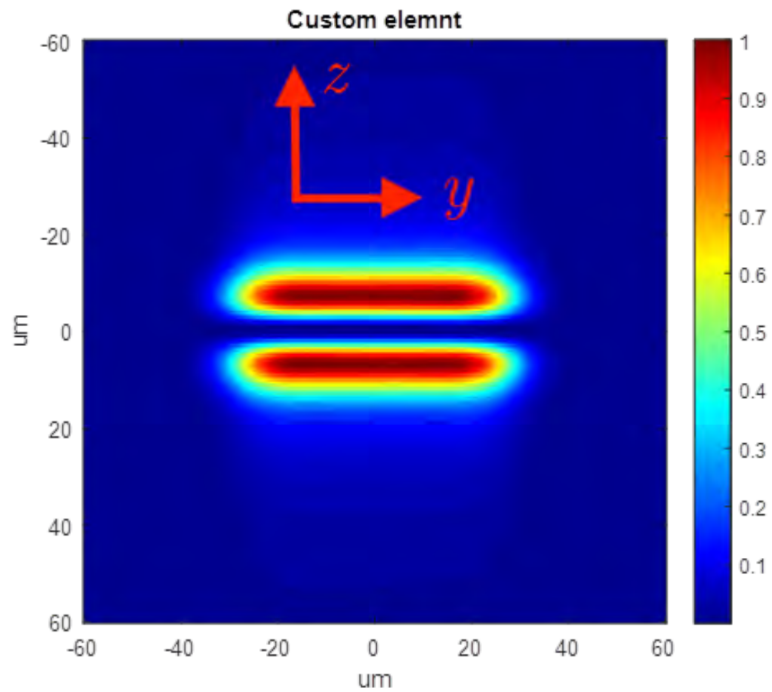

(a) *Beam profile*

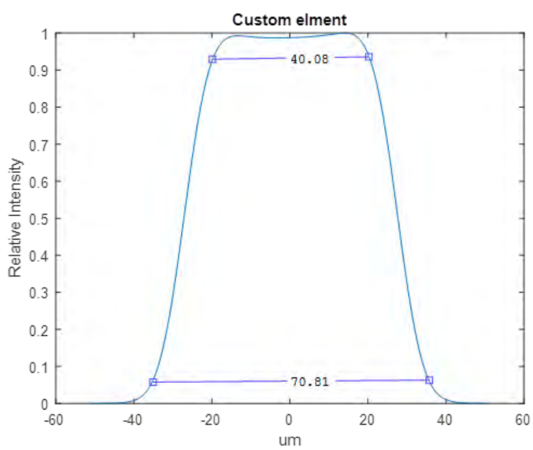

(b) y *direction*

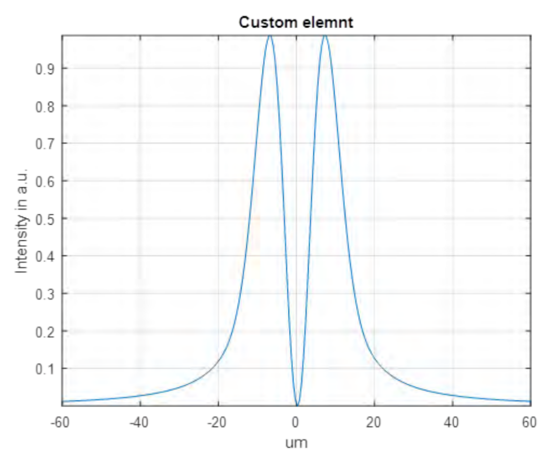

(c) z *direction*

Figure 2.3: *Top-hat potential. The image was provided by Holoor, the manufacturing company.*

Acknowledgements

Bibliography

[1] Immanuel Bloch, Jean Dalibard, and Sylvain Nascimbène. "Quantum Simulations with Ultracold Quantum Gases". In: *Nature Physics* 8.4 (4 Apr. 2012), pp. 267–276. ISSN: 1745-2481. DOI: 10.1038/nphys2259 (cit. on pp. 1, 2).

[2] Richard P. Feynman. "Simulating Physics with Computers". In: *International Journal of Theoretical Physics* 21.6 (June 1, 1982), pp. 467–488. ISSN: 1572-9575. DOI: 10.1007/BF02650179 (cit. on p. 1).

[3] Alexandre Blais et al. "Circuit Quantum Electrodynamics". In: *Reviews of Modern Physics* 93.2 (May 19, 2021), p. 025005. ISSN: 0034-6861, 1539-0756. DOI: 10.1103/RevModPhys.93.025005 (cit. on p. 2).

[4] Xiaoling Wu et al. "A Concise Review of Rydberg Atom Based Quantum Computation and Quantum Simulation*". In: *Chinese Physics B* 30.2 (Feb. 2021), p. 020305. ISSN: 1674-1056. DOI: 10.1088/1674-1056/abd76f (cit. on p. 2).

[5] Colin D. Bruzewicz et al. "Trapped-Ion Quantum Computing: Progress and Challenges". In: *Applied Physics Reviews* 6.2 (May 29, 2019), p. 021314. ISSN: 1931-9401. DOI: 10.1063/1.5088164 (cit. on p. 2).

[6] Immanuel Bloch, Jean Dalibard, and Wilhelm Zwerger. "Many-Body Physics with Ultracold Gases". In: *Reviews of Modern Physics* 80.3 (July 18, 2008), pp. 885–964. ISSN: 0034-6861, 1539-0756. DOI: 10.1103/RevModPhys.80.885 (cit. on p. 2).

[7] Felix Bloch. "Über die Quantenmechanik der Elektronen in Kristallgittern". In: *Zeitschrift für Physik* 52.7 (July 1, 1929), pp. 555–600. ISSN: 0044-3328. DOI: 10.1007/BF01339455 (cit. on p. 2).

[8] Maxime Ben Dahan et al. "Bloch Oscillations of Atoms in an Optical Potential". In: *PHYSICAL REVIEW LETTERS* 76.24 (1996) (cit. on p. 2).

[9] J. Feldmann et al. "Optical Investigation of Bloch Oscillations in a Semiconductor Superlattice". In: *Physical Review B* 46.11 (Sept. 15, 1992), pp. 7252–7255. DOI: 10.1103/PhysRevB.46.7252 (cit. on p. 2).

[10] Markus Greiner, Olaf Mandel, and Tilman Esslinger. "Quantum Phase Transition from a Super¯uid to a Mott Insulator in a Gas of Ultracold Atoms". In: 415 (2002) (cit. on p. 2).

[11] Renate Landig et al. "Quantum Phases from Competing Short- and Long-Range Interactions in an Optical Lattice". In: *Nature* 532.7600 (7600 Apr. 2016), pp. 476–479. ISSN: 1476-4687. DOI: `10.1038/nature17409` (cit. on p. 2).

[12] Sebastian Krinner et al. "Observation of Quantized Conductance in Neutral Matter". In: *Nature* 517.7532 (7532 Jan. 2015), pp. 64–67. ISSN: 1476-4687. DOI: `10.1038/nature14049` (cit. on pp. 2, 3).

[13] Moritz Fontboté Schmidt. "Towards a Uniform Two-Dimensional Channel for Transport Experiments with Ultracold Gases". ETH Zürich, Feb. 17, 2021 (cit. on pp. 4, 7, 9).

[14] Bahaa E. A. Saleh and Malvin Carl Teich. "Fourier Optics". In: *Fundamentals of Photonics*. John Wiley & Sons, Ltd, 1991, pp. 108–156. ISBN: 978-0-471-21374-1. DOI: `10.1002/0471213748.ch4` (cit. on pp. 7, 8).

[15] Ruth Heine. "Digital In-Line x-Ray Holographic Microscopy with Synchrotron Radiation". In: (Jan. 2008) (cit. on p. 8).